Mechanical Programming of Soft Actuators by Varying Fiber Angle

Fionnuala Connolly, Panagiotis Polygerinos, Conor J. Walsh, Katia Bertoldi**

*corresponding author

F. Connolly, Dr. P. Polygerinos, Prof. C. J. Walsh, Prof. K. Bertoldi
School of Engineering and Applied Sciences
Harvard University
Pierce Hall, 29 Oxford Street
Cambridge, MA, 02138, USA
E-mail: walsh@seas.harvard.edu, bertoldi@seas.harvard.edu
Dr. P. Polygerinos, Prof. C. J. Walsh
Wyss Institute for Biologically Inspired Engineering
Harvard University
60 Oxford Street, Cambridge, MA, 02138, USA
Prof. K. Bertoldi
Kavli Institute for Bionano Science and Technology
Harvard University
29 Oxford Street,
Cambridge, MA, 02138, USA

Abstract

In this work we investigate the influence of fiber angle on the deformation of fiber-reinforced soft fluidic actuators. We demonstrate that by simply varying the fiber angle, we can tune the actuators to achieve a wide range of motions, including axial extension, radial expansion, and twisting. We investigate the relationship between fiber angle and actuator deformation by performing finite element simulations for actuators with a range of different fiber angles and we verify the simulation results by experimentally characterizing the actuators. By combining actuator segments in series, we can achieve combinations of motions tailored to specific tasks. We demonstrate this by designing a worm-like soft robot capable of propelling itself through a tube and performing an orientation-specific peg insertion task at the end of the tube. Understanding the relationship between fiber angle and motion of these soft fluidic actuators enables rapid exploration of the design space, opening the door to the iteration of exciting soft robot concepts such as flexible and compliant endoscopes, pipe inspection devices and assembly line robots.

Introduction

In recent years, significant attention has been devoted to the study of soft, fluidic actuators, because of their compliance, easy fabrication, and ability to achieve complex motions with simple control inputs.[1-6] These unique capabilities have led to a variety of innovative potential applications in the areas of medical devices,[7,8] search and rescue devices[9] and assistive robots.[10] One of the most well-known and widely-used pneumatic soft actuators is the McKibben actuator,[11-13] which upon pressurization produces a simple axial contraction and radial expansion motion. This actuator has been studied in detail and has been shown to have many uses. [14-16] However, in order to increase the applicability of soft robots, it is desirable to have access to a library of actuators capable of producing a much wider range of motions. In an effort to increase functionality in soft actuators, multiple McKibben actuators have been combined to produce more complex twisting motions.[7,17] Furthermore,

bending motions have been achieved using PneuNets[2-5] and flexible microactuators (FMAs),[18] and a wider range of motions, including extension, twisting and bending, has been demonstrated by using fillers (paper or fabric) in elastomer composites,[4] fiber-reinforced elastomers,[18] and combinations of elastomers with different stiffnesses.[19] However, in order to simplify and accelerate the design of soft robots, there is still a need to develop actuators which can be easily fabricated and designed, easily programmed to produce a wide range of motions and which can be used as building blocks to realize more complex motions, such as locomotion and burrowing.

We looked to nature for inspiration for the realization of such actuators and noted that fiber-reinforced structures are ubiquitous. For example, nemertean and turbellarian worms have an outer layer of helically arranged collagen fibers to limit the elongation and contraction of the worm's body,[20,21] and the walls of arteries are strengthened with a helical arrangement of collagen fibrils.[22] Furthermore, fiber-reinforced structures in nature often function as actuators. Examples include the body of the earthworm,[23] the tube feet of starfish,[24] and soft muscular systems of the human body, such as the heart.[7] Furthermore, we notice that the nonlinear theory of anisotropic tubes[25-28] and, more recently, simple kinematics models, [29,30] have shown that pressurized fiber-reinforced hollow cylinders are capable of many motions, including axial extension, radial expansion and twisting.

In this paper, we aim to design a mechanically programmable soft actuator whose response can be tuned via how fibers are oriented in its construction. We explore numerically and experimentally the response of fluidic-powered cylindrical elastomeric actuators, with fibers wound in a helical pattern around the outside of the actuator, as shown in Figure 1a and 1c. While previous work has demonstrated that this type of fiber-reinforced actuator is capable of many types of motions,[7,8,11-18] here we study in detail the effect of fiber angle (the angle between the horizontal axis and the fiber) on actuator motion. Our results indicate that by simply varying the fiber angle, we can design actuators which change in length, change in radius, and twist about their axis, as shown in Figure 1b. We also

demonstrate that by using multiple families of fibers (that is, fibers arranged at different angles), we can expand the actuator design space and have greater flexibility in the type of actuator we can create. We show that these systems can be efficiently designed using numerical simulations, which enable rapid exploration of the design space. Furthermore, by combining actuator segments in series, as shown in Figure 1d for example, we can achieve combinations of motions tailored to specific tasks, such as peristaltic locomotion and burrowing.

Results and Discussion

To characterize the effect of fibers on the response of the actuators, we begin by studying them numerically using finite element analysis. Such an approach facilitates accurate modeling of the system, incorporating material properties and the effect of the fiber reinforcement. It also enables much more rapid exploration of the design space, compared with fabricating and experimentally characterizing multiple actuators and therefore can be effectively used to design actuators tailored to specific tasks. We used the commercial finite element package Abaqus, version 6.12-1 (SIMULIA, Providence, RI), to run simulations for actuators with a range of different fiber angles, varying from 0° (circumferential fibers) to 90° (axial fibers) (see Supplementary Video S1; see also Supplementary Data for details of how the simulations were performed). During the simulations, we monitored: (i) the change in the radius of the actuator (b/B), (ii) the change in length of the actuator (λ_z =l/L) and (iii) the amount by which the actuator twists about its longitudinal axis (τ) (see Supplementary Data for details on how to extract these quantities from the simulations). We first focus on actuators with a single family of fibers (that is, all fibers have the same orientation) and in Figure 2a we plot λ_z, b/B and τ as a function of the applied pressure for fiber angles varying from α=0° to α=90°. As expected, for α=0°, corresponding to circumferential fibers, the motion of the actuator is constrained only in the radial direction, so we see in the plot of axial extension versus pressure that maximum axial extension occurs for this angle. As α is increased from 0°, radial expansion increases and axial extension decreases until

finally, at α=90° (axial fibers), we have maximum radial expansion and no axial extension. We also see that for fiber angles in the 50° to 90° range, the axial stretch is non-monotonic, as the length of the actuator first decreases and then increases as pressure increases. Finally, by plotting twist per unit length as a function of pressure, we note that at 0° and 90°, the fibers are arranged symmetrically, so there is no twist about the axis. We also see the unintuitive result that twist peaks around 30°.

To verify the finite element results, we compared numerical predictions and experimental data for two actuators characterized by α=–3° and α=70° (see Supplementary Video S2). From the finite element analysis, we expect that these actuators will exhibit contrasting behavior upon pressurization. Upon completion of the fabrication (see Supplementary Data for details), we pressurized each actuator to 62.05kPa and took pictures of the actuator during the loading process. By tracking markings on the actuator (see Figure 2b and 2c), we could analyze the change in radius and length. To obtain values for the twist, we placed a camera underneath the actuator, and used markings to track the center and four points on the circumference of the bottom of the actuator. In the same way as for the finite element simulations, we plotted the axial stretch, circumferential stretch and twist per unit length, as functions of pressure (see Supplementary Data for details). The results are reported in Figure 2d. In the case of α=–3°, we see excellent agreement between experimental and numerical results. For α=70°, the match is very good at lower pressures, with some deviation at higher pressures due to the highly nonlinear response exhibited by the actuator. In particular, for α=–3° we see that the actuator twists about its axis and extends axially, with little change in the radial dimension. In contrast, for α=70° the actuator twists, expands radially, and undergoes slight axial contraction in response to pressurization. Finally, we note that the discrepancies between the numerical and experimental results are likely due to imperfections in the experiments, and end effects which lead to non-uniform deformations. Having verified the finite element results, we can use the graphs in Figure 2a to design an actuator which maximizes or minimizes extension, expansion or twist. Also, by combining the results from the three

graphs, we can design actuators with specific characteristics, such as an actuator which maximizes twist while minimizing change in radius, or one which maximizes twist and extension.

Although varying the fiber angle of an actuator yields a range of different motions, there are some motions which are more difficult to achieve than others. For example, a pure extending actuator requires a fiber angle of 0°, but achieving this in practice is difficult due to variations in the fabrication process. To overcome this issue, we can add a second family of fibers to the first one. This second family of fibers can be arranged at any angle, leading to a variety of different motions that can be achieved. However, note that if we arrange the two families of fibers symmetrically, there is no twist; the actuator purely extends or expands. We demonstrate this by characterizing an actuator with fibers arranged at α_1=3° and α_2= -3° (see Supplementary Videos S3 and S4). We see in Figure 3a that the behavior in the axial and radial directions is very similar to the case with only one family of fibers (axial extension and slight radial expansion) but now the new family of fibers cancels the twist.

As well as yielding an actuator that does not twist, adding a second family of fibers also expands the design space for this class of actuators. For instance, we can fabricate multiple actuators which have similar twist per unit length as a function of pressure, but different behavior in the axial and radial directions (see Supplementary Videos S5 and S6). We performed a range of finite element simulations and identified a pair of actuators which exhibit this behavior: an actuator with fibers at α_1=17° and α_2= -67°, and one with fibers at α_1=60° and α_2= -11°. In Figure 3b, we compare the response, both experimental and numerical, of these two actuators. We see that the two actuators have almost the same curve for twist as a function of pressure and neither sees much change in radius. However, one actuator extends upon pressurization, while the other contracts. So we see that adding an extra family of fibers expands the design space, giving us greater flexibility in the type of actuator we can create.

The actuators presented here have potential to be used in a wide variety of applications. For example, we can combine them to fabricate a device capable of propelling itself through a tube with a 90° bend in it and performing an orientation-specific peg insertion task at the end (see Supplementary Video S7). To design such a device, we took inspiration from the peristaltic locomotion of the earthworm.[21] The earthworm uses longitudinal and circumferential muscles to contract the segments of its body sequentially, enabling it to move forward. Therefore, we assembled four actuators in series, as shown in Figure 4a, with segments 1, 2, and 3 responsible for propelling the device through the tube and segment 4 designed to twist the prongs into the holes.

More specifically, actuator segments 1 and 3 were required to expand and anchor the device in the tube, so we chose to arrange the fibers symmetrically at 70° and -70° to achieve a balance between maximum expansion and ease of fabrication. To choose the dimensions of the actuators, we took advantage of finite element analysis. Considering a tube with an inner diameter of 13 mm, we performed a range of finite element simulations and found that an actuator with an outer diameter of 8mm, a wall thickness of 1mm and fibers symmetrically arranged at angles of 70° and -70° would expand to give an outer diameter of 14.5mm at a pressure of 100kPa, and this would be sufficient to act as an anchor. In contrast to the anchoring segments, the function of segment 2 was to achieve extension and move the device forward, so we arranged the fibers symmetrically at 7° and -7°. The actuation sequence required for forward locomotion is shown in Figure 4b. When we actuate segment 1, it expands and anchors the device in the tube. Segment 2 extends, to move the device forward. Segment 3 expands to anchor the device in the forward position, and we can then depressurize segments 1 and 2. It is key to note that, since all of the segments are completely soft, the bend in the tube is easily negotiated (see Figure 4b-center). This would be much more difficult to achieve if rigid components were used.

When the device reaches the end of the tube, we then want it to insert the two prongs at its front into two holes. Since the prongs are typically misaligned (see Figure 4c), we actuate segment 4, whose fibers are arranged asymmetrically, at an angle of 10°, to achieve a balance of extension and twisting. As shown in Figure 4c, the prongs easily twist into the holes and we can use segments 1, 2, and 3 to adjust the position of the device, if necessary. Since the device has intrinsic passive compliance, even if the front segment is not exactly centered in the tube, the prongs still find their way into the holes.

Conclusion

In summary, we have shown that by simply varying the fiber angle of fluidic-powered fiber-reinforced soft actuators, we can tune their response to achieve a wide range of motions. Finite element simulations accurately model the relationship between fiber angle and output motion and we can use the results of these simulations to guide the design of soft actuators and greatly accelerate the design process. Future challenges in this area will include optimization of the simulations to reduce computation time whilst still maintaining accuracy, inclusion of dynamic effects in the simulations, refinement of the fabrication procedure and the development of analytical models for use in real-time controllers. We highlight the utility of knowledge gained from the simulations by mechanically programming multiple soft actuator segments and combining them in series to create a worm-like soft robot that can navigate through a pipe and complete a simple insertion task. The ability to understand how tailoring of the fiber angle influences the motion of the soft actuators enables rapid exploration of the design space for this class of soft actuators and the iteration of exciting soft robot concepts such as flexible and compliant endoscopes, pipe inspection devices and assembly line robots, to name but a few.

Acknowledgements

This work has been supported by Harvard MRSEC through Grant No. NSF DMR-1420570. KB acknowledges support from NSF through Grant No. CMMI-1149456 (CAREER) and by the Wyss

Institute through the Seed Grant Program. The authors are grateful to Dr. Kevin Galloway, Johannes Overvelde, Sicong Shan and Dr. James Weaver for assistance with actuator fabrication, FE simulations, Matlab tracking code and 3d printing, respectively.

Author Disclosure Statement

No competing financial interests exist.

References

[1] Wakimoto S, Suzumori K, Ogura K. Miniature pneumatic curling rubber actuator generating bidirectional motion with one air-supply tube. Adv Robot 2011**;** 25(9-10):1311-1330.

[2] Ilievski F, Mazzeo AD, Shepherd RF, Chen X, Whitesides GM. Soft robotics for chemists. Angew Chem Int Ed 2011; 50(8):1890-1895.

[3] Martinez RV, Branch JL, Fish CR, Jin L, Shepherd RF, Nunes RMD, Suo Z, Whitesides GM. Robotic tentacles with three-dimensional mobility based on flexible elastomers. Adv Mater 2013; 25(2):205-212.

[4] Martinez RV, Fish CR, Chen X, Whitesides GM. Elastomeric origami: Programmable paper-elastomer composites as pneumatic actuators. Adv Funct Mater 2012; 22(7):1376-1384.

[5] Shepherd RF, Stokes AA, Nunes RMD, Whitesides GM. Soft machines that are resistant to puncture and that self seal. Adv Mater 2013; 25(46):6709-6713.

[6] Majidi C. Soft robotics: A perspective-Current trends and prospects for the future. Soft Robotics 2013; 1(1):5-11.

[7] Roche ET, Wohlfarth R, Overvelde JTB, Vasilyev NV, Pigula FA, Mooney DJ, Bertoldi K, Walsh CJ. A bioinspired soft actuated material. Adv Mater 2014; 26(8):1200-1206.

[8] Polygerinos P, Wang Z, Galloway KC, Wood RJ, Walsh CJ. Soft robotic glove for combined assistance and at-home rehabilitation. Rob Auton Syst 2014 [E-pub ahead of print]; DOI: 10.1016/j.robot.2014.08.014.

[9] Tolley MT, Shepherd RF, Mosadegh B, Galloway KC, Wehner M, Karpelson M, Wood RJ, Whitesides GM. A resilient, untethered soft robot. Soft Robotics 2014; 1(3):213-223.

[10] Sanan S, Ornstein MH, Atkeson CG. Physical human interaction for an inflatable manipulator. Conf Proc IEEE Eng Med Biol Soc 2011**;** 7401-7404.

[11] Schulte HF. The characteristics of the McKibben artificial muscle. *In* The application of external power in prosthetics and orthotics. Natl Acad Sci 1961: 94-115.

[12] Andrikopoulos G, Nikolakopoulos G, Manesis S. A survey on applications of pneumatic artificial muscles. Mediterr Conf Control Automation 2011; 1439-1446.

[13] Chou CP, Hannaford B. Measurement and modeling of McKibben pneumatic artificial muscles. IEEE Trans Rob Autom 1996; 12(1):90-102.

[14] Davis S, Caldwell DG. Braid effects on contractile range and friction modeling in pneumatic muscle actuators. Int J Robot Res 2006; 25(4):359-369.

[15] Zhang Z, Philen M. Modeling, analysis and experiments of inter yarn compaction effects in braided composite actuators. J Compos Mater 2013; 47(25):3211-3225.

[16] Mortier K. Braided pneumatic muscles for rehabilitation apparatus. Masters dissertation. Politecnico di Torino 2014.

[17] Pritts MB, Rahn CD. Design of an artificial muscle continuum robot. IEEE Trans Rob Autom 2004; 5:4742-4746.

[18] Suzumori K, Iikura S, Tanaka H. Flexible microactuator for miniature robots. Proc IEEE Micro Electro Mech Syst 1991; 204-209.

[19] Konishi S, Nokata M, Jeong OC, Kusada S, Sakakibara T, Kuwayama M, Tsutsumi H. Pneumatic micro hand and miniaturized parallel link robot for micro manipulation robot system. IEEE Trans Rob Autom 2006; 1036-1041.

[20] Cowey JB. The structure and function of the basement membrane muscle system in amphiporus lactifloreus (nemertea). Q J Microsc Sci 1952; 93:1-15.

[21] Clark RB, Cowey JB. Factors controlling the change of shape of certain nemertean and turbellarian worms. J Exp Biol 1958; 35:731-748.

[22] Holzapfel GA, Gasser TC, Ogden RW. A new constitutive framework for arterial wall mechanics. J Elast 2000; 61(1):1-48.

[23] Quillin KJ. Kinematic scaling of locomotion by hydrostatic animals: Ontogeny of peristaltic crawling by the earthworm lumbricus terrestris. J Exp Biol 1999; 202(6):661-674.

[24] McCurley RS, Kier WM. The functional morphology of starfish tube feet: The role of a crossed-fiber helical array in movement. Biol Bull 1995; 188(2):197-209.

[25] Adkins JE, Rivlin RS. Large elastic deformations of isotropic materials X. Reinforcement by inextensible cords. Philos Trans R Soc A 1955; 248(944):201-223.

[26] Wang ASD, Ertepinar A. Stability and vibrations of elastic thick-walled cylindrical and spherical shells subjected to pressure. Int J Nonlinear Mech 1972; 7(5):539-555.

[27] Haughton DM, Ogden RW. Bifurcation of inflated circular cylinders of elastic material under axial loading-II. Exact theory for thick-walled tubes. J Mech Phys Solids 1979; 27(5):489-512.

[28] Goriely A, Tabor M. Rotation, inversion and perversion in anisotropic elastic cylindrical tubes and membranes. Proc R Soc London A 2013; 469(2153).

[29] Krishnan G, Bishop-Moser J, Kim C, Kota S. Evaluating mobility behavior of fluid filled fiber-reinforced elastomeric enclosures. Proc ASME Des Eng Tech Conf 2012; 4:1089-1099.

[30] Bishop-Moser J, Krishnan G, Kim C, Kota S. Kinematic synthesis of fiber-reinforced soft actuators in parallel combinations. Proc ASME Des Eng Tech Conf 2012; 4:1079-1087.

Figure 1. Fiber-reinforced soft actuators. a) The actuators consist of an elastomeric matrix surrounded by a helical arrangement of fibers. b) The actuators can expand, extend or twist upon pressurization. c) A combination of finite element modeling and experimental characterization is used to explore the motions that can be achieved. d) Combining actuator segments in series we can achieve combinations of motions tailored to specific tasks. For example, we can combine extending and expanding segments to create a robot capable of navigating through a pipeline.

Figure 2. Actuators with one family of fibers. a) Finite element results showing extension (λ_z), expansion (b/B), and twist per unit length (τ) as a function of the applied pressure for a range of different fiber angles. Note that we define the positive fiber orientation to be in the clockwise direction. Positive fiber orientation induces twist in the counter-clockwise direction (negative twist). However, here we are interested in comparing the magnitude of the twist for different angles, so we plot the magnitude of the twist (rather than magnitude and direction). b) Photographs from experimental characterization (left) and snapshots from finite element simulation (right) for an actuator with fiber angle α=-3°. Both front views (top) and bottom views (bottom) are shown. c) Photographs from experimental characterization (left) and snapshots from finite element simulation (right) for an actuator with fiber angle α=70°. d) Comparison between finite element simulations and experiments for two actuators with fiber angle α=-3° and α=70°. The error bars on the experimental results show the standard deviation from the mean result obtained by pressurizing each actuator three times. As in Figure 2a, the magnitude of the twist is plotted here, rather than magnitude and direction.

Figure 3. Actuators with two families of fibers. a) Photographs from experimental characterization (left), snapshots from finite element simulation (center) and comparison between finite element and experimental results (right) for an actuator with fibers symmetrically arranged at α_1=3° and α_2=-3°.

The error bars show the standard deviation from the mean result obtained by pressurizing each actuator three times. b) Photographs from experimental characterization (left) and snapshots from finite element simulation (right) for an actuator with fibers at α_1=17° and α_2= -67°. c) Photographs from experimental characterization (left) and snapshots from finite element simulation (right) for an actuator with fibers at α_1=60° and α_2= -11°. d) Comparison between finite element and experimental results for an actuator with fibers at α_1=17° and α_2=-67° and an actuator with fibers at α_1=60° and α_2= -11°. The error bars show the standard deviation from the mean result obtained by pressurizing each actuator three times.

Figure 4. Device capable of propelling itself through a tube and performing an orientation-specific task a) Four actuator segments are combined in series to achieve forward locomotion and perform an orientation-specific task. b) Segments 1, 2 and 3 are actuated in sequence to move the device through a bent tube. c) As the device approaches the end of the tube the prongs are not aligned with the holes. Segment 4 is then actuated, extending and twisting the prongs into the holes.

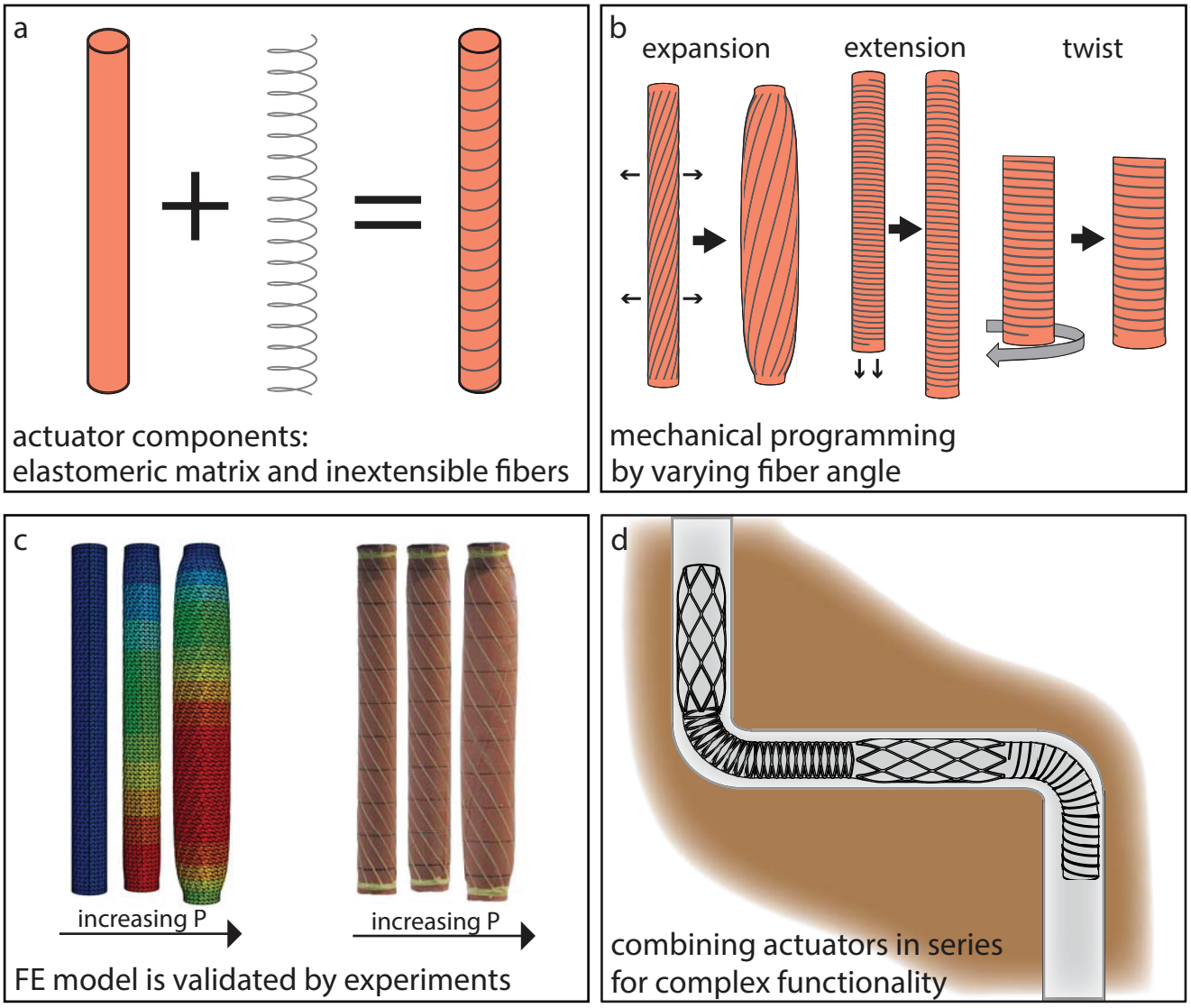
a
actuator components:
elastomeric matrix and inextensible fibers
b
expansion
extension
twist
mechanical programming
by varying fiber angle
c
increasing P
increasing P
FE model is validated by experiments
d
combining actuators in series
for complex functionality

Figure 1

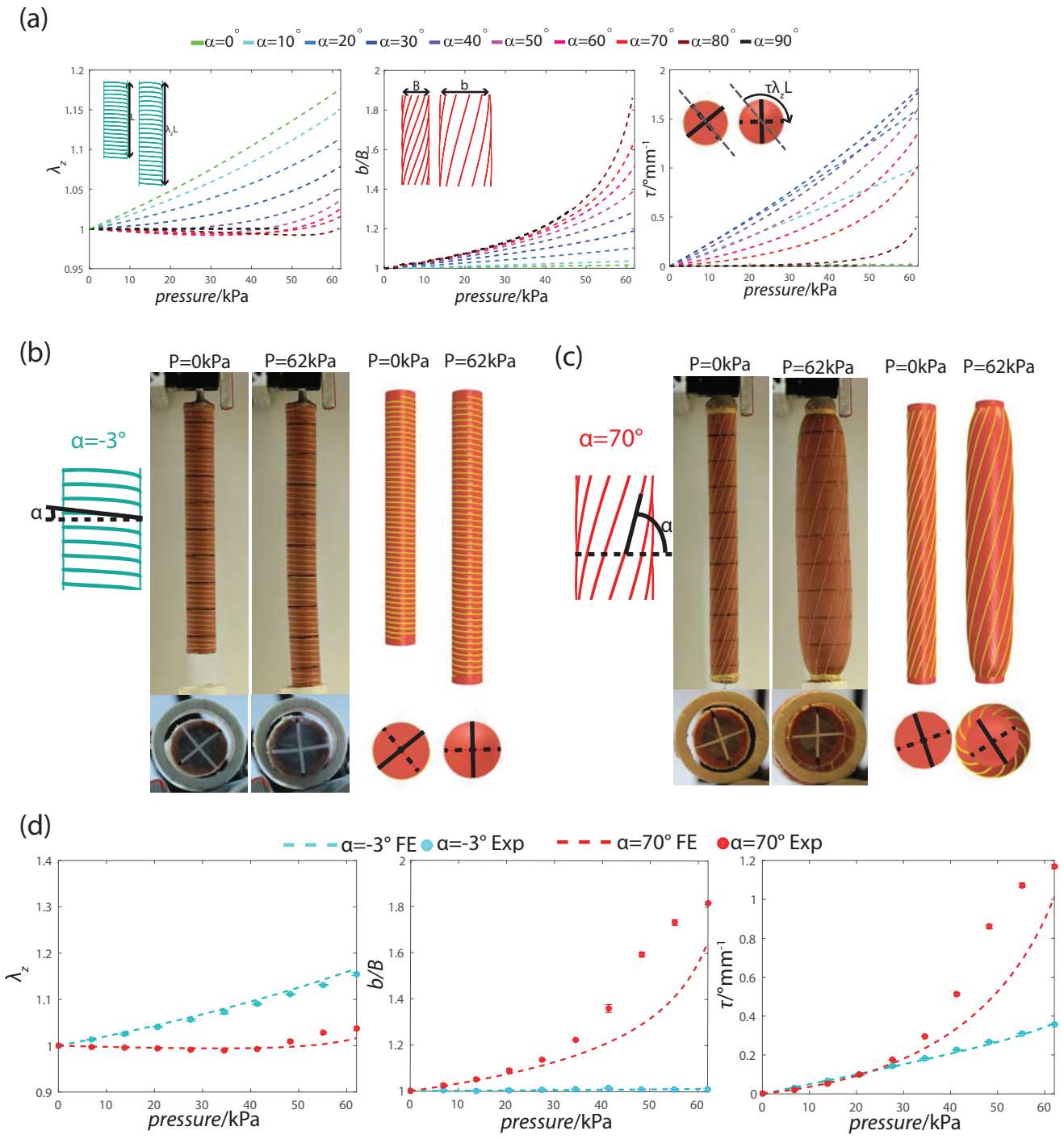
(a)
α=0° α=10° α=20° α=30° α=40° α=50° α=60° α=70° α=80° α=90°
λz
pressure/kPa
b/B
τ/°mm-1
τλz L
(b)
P=0kPa P=62kPa P=0kPa P=62kPa
α=-3°
α
(c)
P=0kPa P=62kPa P=0kPa P=62kPa
α=70°
α
(d)
α=-3° FE α=-3° Exp α=70° FE α=70° Exp
λz
b/B
τ/°mm-1
pressure/kPa

Figure 2

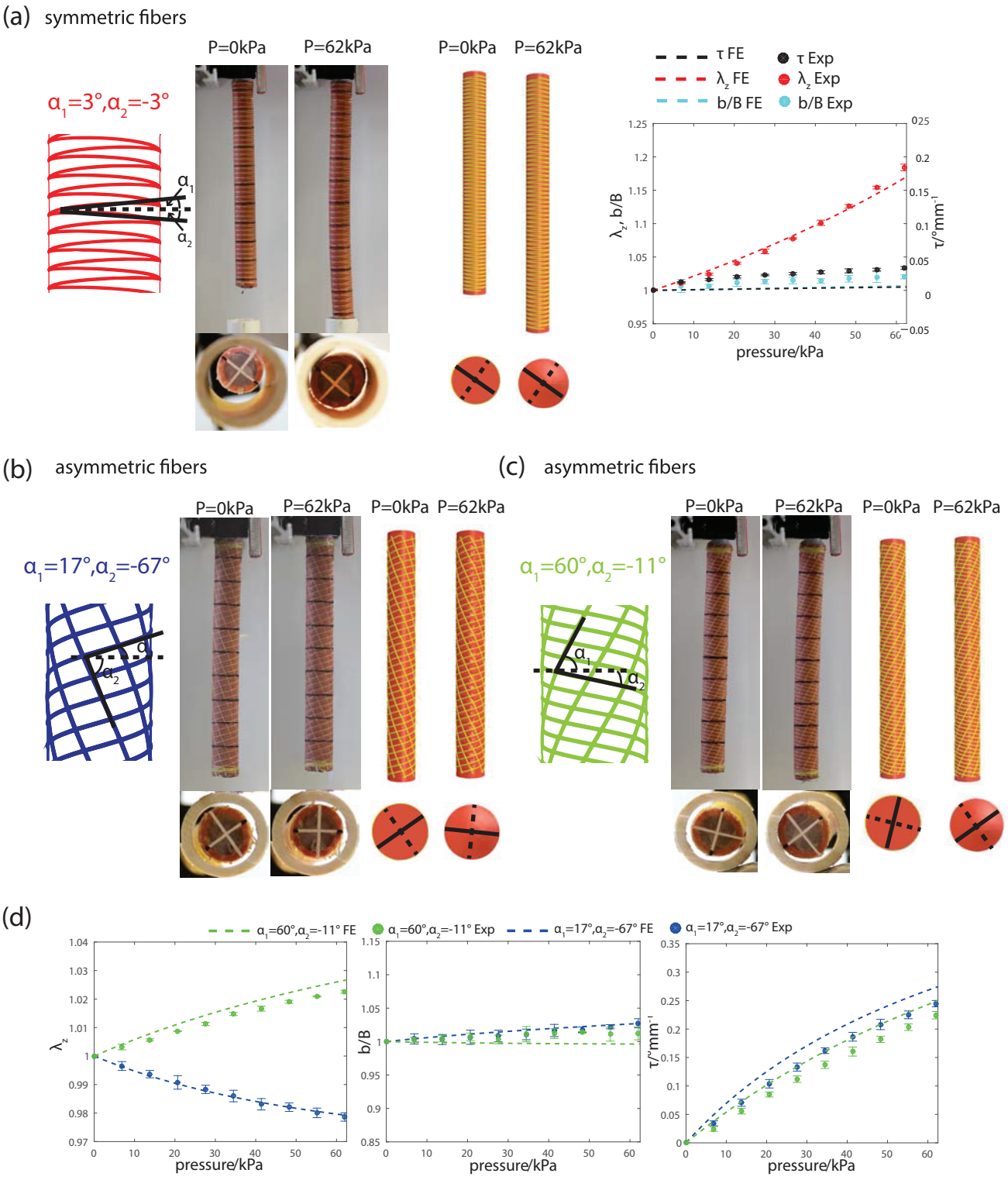
(a) symmetric fibers
P=0kPa
P=62kPa
P=0kPa
P=62kPa
α1=3°,α2=-3°
α1
α2
τ FE
λz FE
b/B FE
τ Exp
λz Exp
b/B Exp
λz, b/B
τ/°mm-1
pressure/kPa
(b) asymmetric fibers
P=0kPa
P=62kPa
P=0kPa
P=62kPa
α1=17°,α2=-67°
α1
α2
(c) asymmetric fibers
P=0kPa
P=62kPa
P=0kPa
P=62kPa
α1=60°,α2=-11°
α1
α2
(d)
α1=60°,α2=-11° FE
α1=60°,α2=-11° Exp
α1=17°,α2=-67° FE
α1=17°,α2=-67° Exp
λz
b/B
τ/°mm-1
pressure/kPa
pressure/kPa
pressure/kPa

Figure 3

(a)

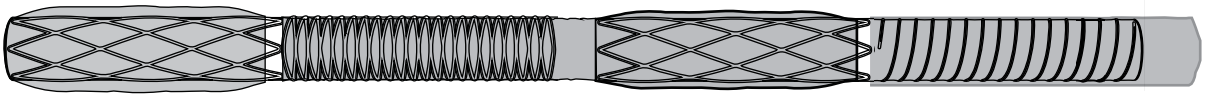

1. expanding segment anchors

2. extending segment advances forward

3. expanding segment anchors

4. twisting/extending segment inserts prongs

(b)

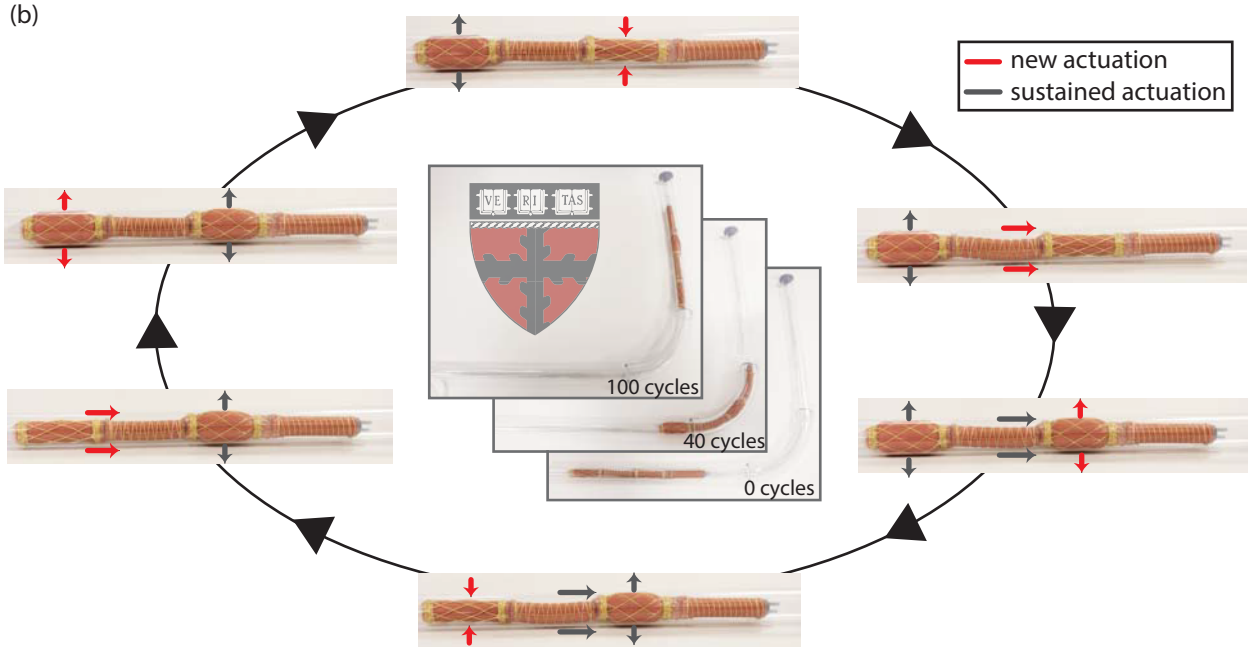

(c)

Figure 4

Address correspondence to:

Prof. Conor J. Walsh
School of Engineering and Applied Sciences
Harvard University
Pierce Hall, 29 Oxford Street
Cambridge, MA, 02138, USA
E-mail: walsh@seas.harvard.edu

Prof. Katia Bertoldi
School of Engineering and Applied Sciences
Harvard University
Pierce Hall, 29 Oxford Street
Cambridge, MA, 02138, USA
E-mail: bertoldi@seas.harvard.edu